

RESEARCH ARTICLE

# Biological and structural effects after intraosseous infiltrations of age-dependent platelet-rich plasma: An in vivo study

Diego Delgado<sup>1</sup>  | Ane Garate<sup>1</sup> | Pello Sánchez<sup>1</sup> | Ane Miren Bilbao<sup>2</sup> | Gontzal García del Caño<sup>3</sup>  | Joan Salles<sup>4,5</sup> | Mikel Sánchez<sup>1,2</sup> 

<sup>1</sup>Advanced Biological Therapy Unit, Hospital Vithas San José, Vitoria-Gasteiz, Spain

<sup>2</sup>Arthroscopic Surgery Unit, Hospital Vithas San José, Vitoria-Gasteiz, Spain

<sup>3</sup>Department of Neurosciences, Faculty of Pharmacy, University of the Basque Country (UPV/EHU), Vitoria-Gasteiz, Spain

<sup>4</sup>Department of Pharmacology, Faculty of Pharmacy, University of the Basque Country (UPV/EHU), Vitoria-Gasteiz, Spain

<sup>5</sup>Centro de Investigación Biomédica en Red de Salud Mental (CIBERSAM), Madrid, Spain

#### Correspondence

Mikel Sánchez, Arthroscopic Surgery Unit, Hospital Vithas San José 4. floor, C/Beato Tomás de Zumarraga 10, 01008 Vitoria-Gasteiz, Spain.

Email: [mikel.sanchez@ucattrauma.com](mailto:mikel.sanchez@ucattrauma.com)

#### Funding information

Eusko Jaurlaritza, Grant/Award Number: HAZITEK; Provincial Council of Alava, Grant/Award Number: AlavalInnova

## Abstract

Platelet-rich plasma (PRP) is an increasingly widespread treatment for joint pathologies. Its characteristics and administration route are variables that may influence the clinical outcome. The aim of this in vivo study was to analyze in aged rats the biological and structure effects of intraosseous infiltrations of two different types of PRP obtained from young and old donors. During 6 months intraosseous infiltrations were performed and 4 days after the last infiltration, animals were sacrificed, and bones were extracted for micro-computed tomography (micro-CT) and histological analysis. Molecular composition of the PRP of aged donors presented higher levels of proinflammatory molecules. The histological studies showed a greater cellularity of bone marrow in groups treated with PRP. Concerning micro-CT analysis, young PRP showed a better femoral bone structure according to values of percentage of trabecular bone, trabecular space, trabecular density, and subchondral bone plate volume. In summary, this study has demonstrated that intraosseous infiltrations of PRP from young donors prevent from age-related bone degeneration. This treatment could stimulate the biological processes that maintain homeostasis and bone structure and avoid osteoarticular pathologies.

#### KEY WORDS

bone marrow, growth factors, intraosseous injections, platelet-rich plasma, subchondral bone

## 1 | INTRODUCTION

During the last recent years, the approach to joint pathologies has been evolving towards a more global vision in which the joint is considered a single entity. This model considers a holistic concept that encompasses different tissues such as cartilage, synovial membrane, and subchondral bone. The interaction of these structures is not static but dynamic, in which each element influences the rest and vice versa. These all together contribute to the maintenance of joint homeostasis or on the contrary, to the breakup of that balance, generating favorable conditions for joint

degeneration.<sup>1</sup> Several studies have demonstrated the on cartilage by diffusing molecules from it to the deepest layers of the cartilage. This diffusion is greater in pathologies such as osteoarthritis when fissures and microcracks increment the number and size of molecules that pass through the layers.<sup>2</sup> In addition, lesions produced in the subchondral bone can generate neovascularization and nerve growth favoring an inflammatory environment and altering its biology and structure.<sup>3</sup> Therefore, the similar influence that joint tissues have on triggering degenerative pathologies in the knee means that all of them must be considered as therapeutic targets.

Normally, the treatments in patients with joint pathologies include intra-articular injections of various products such as hyaluronic acid, stem cells or platelet-rich plasma (PRP). The latter is obtained from the patient's own blood and comprises of a biological product composed of plasma with a platelet concentration higher than in blood, obtaining a cocktail of bioactive molecules.<sup>4</sup> By means of intra-articular PRP injections, its biological action affects only the cells and tissues present in the synovial membrane and superficial layers of the cartilage. Although this therapy showed efficacy in diseases such as osteoarthritis,<sup>5,6</sup> it can be conditioned both by the degree of severity of the pathology and by different PRP variables such as preparation, donor, patient, characteristics, or administration route. Therefore, extending the range of action of PRP by its injection into the subchondral bone using intraosseous infiltrations could be a therapy not only to treat severe degenerative pathologies but also to maintain homeostasis of the joint due to the connection between this tissue and cartilage as mentioned above.<sup>7</sup> Although several studies have achieved promising clinical results in patients with severe osteoarthritis,<sup>8,9</sup> the biological and structural effects of this type of injections have not yet been evaluated.

In addition, maintaining the homeostasis of the bone marrow is also important for an adequate bone mass and structure since breaking that balance can lead to the development of osteoarticular pathologies.<sup>10</sup> Normal physiological processes such as aging can also affect the proper biological condition of the bone marrow and treatments that prevent its deterioration can improve the quality of life of patients.<sup>11</sup> The biological stimuli produced by PRP could also affect the bone marrow and consequently improve its activity in functions such as bone regulation.

The modulation of PRP efficacy by adding this route of administration can also be enhanced by acting on the composition of the PRP. Considering that PRP is an autologous therapy, the characteristics of each patient are relevant to achieve apposite results with the treatment. Although currently modifying its molecular composition is very difficult, it is possible to compare different PRP based on the type of donor population. According to several studies, the composition of plasma varies when comparing young with the elderly population and this change in molecular levels could mean a change in clinical efficacy.<sup>12</sup> Indeed, several studies showed how a greater presence of proinflammatory molecules in PRP can affect their biological effects on cells and tissues.<sup>13,14</sup>

Keeping all this in mind, the aim of this study is to analyze the bone structural effects after intraosseous PRP infiltrations into the bone marrow, and the differences in applying age-dependent PRP.

## 2 | METHODS

### 2.1 | Animals

In this study, 24 aged Wistar rats (18 months of age) were used. Animal handling and surgical procedures were carried out according to the directive of the European Parliament and Council of the European Communities (2010/63/UE) and the Spanish legislation (RD 1201/2005 and Law 32/2007). The protocol (M20\_2017\_57) of this study was approved

by the local ethics committee. Animals were quarantined for at least 1 week prior to the study. They were housed under standard conditions and had "ad libitum" access to water and standard laboratory rodent diet.

Animals were divided into four groups: control group (C), saline group (S), young PRP group (Y-PRP), and aged PRP group (A-PRP). During 6 months six bilateral infiltrations were conducted into the femurs on a monthly basis for S, Y-PRP and A-PRP groups. PRP was obtained from 3-month-old (young) and 18-month-old (aged) donors and it was administered to Y-PRP and A-PRP groups, respectively. For this reason, Wistar rats of 3 and 18 months were included during the study to use them as PRP donors. Saline group received intraosseous saline injections while the control group underwent the same surgery without receiving any treatment.

### 2.2 | PRP preparation

Each day of the intervention, both pools of PRP (young and old) were prepared to extract up to a total blood volume of 20 mL from each group. Each donor group was composed of four animals, from which up to 5 mL were extracted to achieve the final volume of 20 mL for each pool. Blood was withdrawn by cardiac puncture into 5 mL tubes soaked with ethylenediaminetetraacetic acid to prevent coagulation. Blood was centrifuged for 8 min at 300g at room temperature. After centrifugation, three layers were obtained, plasma, buffy coat, and red blood cells. Plasma was collected avoiding the leukocyte layer in order to prepare at least 3 mL of PRP to perform intraosseous infiltrations. Both PRP pools were prepared each day of the intervention, with a total of 6 pools of each donor group throughout the study. The number of erythrocytes, leukocytes, and platelets from PRP, were assessed using a hematology analyzer. The analysis of both PRPs was extended by analyzing biomolecules. For these analyses, samples from each pool were collected and duplicate analyses were performed. After determining protein concentration using the BCA protein quantification kit (Abcam, Cambridge, UK; BD Transduction Laboratories, San Diego, CA), PRP samples from young and aged donors were assayed in duplicate using the Proteome Profiler Ray XL Cytokine Array Kit as per the manufacturer's instructions (R&D Systems, MN). Briefly, membranes spotted with capture antibodies against 79 different rat cytokines printed in duplicate were incubated with 6.5 mg PRP protein in 1.5 mL overnight at 4°C. Thereafter, the horseradish peroxidase-conjugated detection antibody cocktail was added for 1 hour at room temperature and signals were visualized by exposing X-ray films to enzymatic chemiluminescence for 10 minutes. Films were scanned in transmission mode and digitized in 16-bit grayscale and 300 dpi resolution. The integrated optical density (arbitrary units) of each spot was quantified by densitometry using the ImageJ image analysis software (ImageJ; NIH, Bethesda, MD).

### 2.3 | Treatment administration

Infiltrations were bilateral in the distal epiphyso-metaphysis of the femur, performed once a month up to a total of six infiltrations and

under isoflurane inhalation anesthesia. Briefly, the femur was located by palpation and an incision was conducted over it. After separate the muscle layers, the femur was exposed and drilling was performed into the distal part of the femur to introduce the needle and carry out the intraosseous injection of young PRP, aged PRP, or saline. In each femur, 200 µL of the product were infiltrated depending on the study group. Finally, the wound was closed, and the good condition of the animals was evaluated (Supporting Information Video 1). During the study mobility and weight control were performed before and after each infiltration. Animals had a good recovery after each operation and none of the rats suffered significant weight variations.

After the intervention and 24 hours later the animals received subcutaneous buprenorphine (0.05 mg/kg). Four days after the last infiltration, animals were anesthetized with ketamine and xylazine prior to sacrifice (80 and 10 mg/kg, respectively). One of the femurs of each rat was removed and preserved in formaldehyde for the micro-computed tomography (micro-CT). The same femurs together with the vastus lateralis muscle were also evaluated by histological analysis. The contralateral femurs that were not used for the analyses were preserved in formaldehyde and kept and stored as a back-up.

## 2.4 | micro-CT analysis

Rat femurs three-dimensional (3D) tomographic images were acquired using X-ray micro-CT (MicroCAT II; Siemens Preclinical Solutions, Knoxville, TN) with the following parameters: 80 kVp X-ray source voltage, 500 µA current, and 2000-ms exposure time per projection. Seven hundred micro-CT projections were acquired with isotropic 20-µm voxel size and a resolution of 768 × 768 pixels. micro-CT images were automatically reconstructed using the Cobra software (Exxim Computing Corporation, CA). 3D bone images were rendered using the Amira 3D Software for preclinical analysis (Thermo Fisher Scientific, MA).

To perform the bone histomorphometry analysis, three regions of interests (ROIs) containing the bone epiphysis, metaphysis and diaphysis were defined from the original scan at a resolution of 20 microns. The analysis of bone histomorphometry in each ROI was carried out using a plugin developed for Fiji/ImageJ, an open-source Java-based image processing software.<sup>15</sup> The plugin was developed by the Imaging Platform at the Center for Applied Medical Research (CIMA). Histomorphometry parameters related to cortical bone, trabecular bone, and subchondral plate were calculated using BoneJ version 1.4.2.<sup>16</sup>

## 2.5 | Histological analysis

For these analyses, the same femurs that were previously used in the micro-CT analysis. The femurs and vastus lateralis were fixed in 4% paraformaldehyde for at least 24 h. In the case of the femurs, once fixed, they were decalcified by soaking them in 10% EDTA (0.8M) at pH 6.5 and room temperature. The EDTA solution was replaced every

2 days for 4 weeks. Next, all samples were dehydrated in an increasing series of graded alcohols, rinsed in xylene substitute and embedded in paraffin, cutting the obtained blocks longitudinally. The resulting sections from the femur were stained with hematoxylin and eosin and Masson's trichrome. Sections from vastus lateralis were stained with Sirius Red in order to evaluate myofiber collagen content.

The samples were examined by conventional optical microscopy (Axio Vert; Carl Zeiss Microscopy GmbH, Germany), and photographed with a digital camera (AxiCam ICc1; Carl Zeiss Microscopy GmbH). The percentage of cellularity of the femur diaphysis respect total area and the percentage of collagen in muscle respect total area were analyzed manually and/or semi-automatically using the ImageJ software v.1.4 (NIH). In the case of bone marrow cellularity, cell nuclei (purple) were quantified and compared to the number of adipocytes or adipogenesis (white). Cartilage present in femur epiphysis was analyzed by using the International Cartilage Repair Society (ICRS) scoring system (Mainil-Varlet).

## 2.6 | Statistical analysis

Comparisons were performed by analysis of variance (ANOVA). The normal distribution of samples was assessed by the Shapiro-Wilk test and homogeneity of variance by the Levene test. In case the data did not fit the normal distribution or the variances were not homogeneous, the nonparametric Kruskal-Wallis one-way ANOVA was applied. Data were considered statistically significant when *P* values were less than .05. Statistical analysis was performed with PASW Statistics 18.0 (SPSS, Chicago, IL).

# 3 | RESULTS

## 3.1 | PRP characterization

There were no significant cellular differences between the PRP of the group Y-PRP and A-PRP. Both PRPs did not have erythrocytes (Y-PRP:  $0.02 \times 10^6 \pm 0.01$  cells/µL; A-PRP:  $0.02 \times 10^6 \pm 0.01$  cells/µL), leukocytes below baseline (Y-PRP:  $0.11 \times 10^3 \pm 0.11$  cells/µL; A-PRP:  $0.05 \times 10^3 \pm 0.04$  cells/µL), and the average enrichment in platelets was 1 to 1.5 times the concentration of platelets compared with blood (Y-PRP:  $979.0 \times 10^3 \pm 253.14$  cells/µL; A-PRP:  $11149.00 \times 10^3 \pm 431.34$  cells/µL). According to the PAW classification system, the PRP used in this study was P1-x-B $\beta$ .<sup>4</sup> Concerning molecular composition. Thirty-five molecules were detected of which CCL21, CSCL5, and VCAM-1 were significantly higher in the PRP of elderly donors (*P* < .05). All values are shown in Figure 1.

## 3.2 | Histological analysis

No group showed differences (*P* > .05) in the histological analysis of cartilage (Figure 2) regarding surface, matrix, cell distribution, cell

Coordinate	Analyte	Y-PRP Group (mean ± sd)	A-PRP Group (mean ± sd)	p value
A03-04	Adiponectin	2048.66 ± 115.41	2560.14 ± 187.24	0.081
A05-06	CCL2	99.36 ± 37.42	104.64 ± 13.77	0.875
A09-10	CCL5	181.67 ± 17.26	464.54 ± 154.21	0.124
A11-12	CCL11	420.65 ± 24.06	297.97 ± 52.37	0.094
A17-18	CCL21	164.42 ± 29.76	534.01 ± 4.77	0.003*
A19-20	CCL22	152.64 ± 23.13	98.53 ± 25.94	0.161
A21-22	Clusterin	61.19 ± 33.90	115.37 ± 16.06	0.177
B09-10	CXCL7	158.76 ± 75.17	145.53 ± 32.63	0.838
B11-12	CCN1	18.11 ± 25.61	36.79 ± 12.91	0.445
B13-14	Cystatin C	224.97 ± 84.98	278.34 ± 3.99	0.467
B15-16	DPPIV	97.77 ± 32.47	118.74 ± 2.02	0.468
B21-22	Endostatin	307.37 ± 69.24	460.88 ± 32.40	0.105
C03-04	Fetuin A	236.42 ± 35.92	359.45 ± 61.04	0.135
C11-12	Fibulin 3	88.58 ± 50.50	93.87 ± 54.37	0.933
C13-14	Flt-3 Ligand	210.33 ± 74.98	100.33 ± 6.67	0.176
D03-04	Hepassocin	51.51 ± 72.85	114.18 ± 1.31	0.349
D05-06	HGF	93.75 ± 48.96	90.97 ± 2.10	0.939
D07-08	ICAM-1	18.33 ± 25.92	89.46 ± 51.87	0.225
D11-12	IGF-I	1170.88 ± 430.14	848.54 ± 182.50	0.432
D13-14	IGFBP-2	791.28 ± 274.22	793.19 ± 61.62	0.991
D15-16	IGFBP-3	731.09 ± 246.53	991.62 ± 61.02	0.284
D17-18	IGFBP-5	54.44 ± 76.99	110.11 ± 29.49	0.442
D19-20	IGFBP-6	504.17 ± 261.05	675.82 ± 174.66	0.522
E17-18	Jagged 1	18.18 ± 25.71	28.42 ± 40.19	0.785
E21-22	Lipocalin-2	155.65 ± 54.14	367.59 ± 138.22	0.18
E23-24	CXCL5	464.33 ± 50.85	1532.18 ± 151.03	0.011*
F03-04	MMP-2	71.77 ± 39.29	69.56 ± 37.96	0.954
F11-12	CCN3	136.75 ± 90.18	93.9 ± 0.71	0.567
F17-18	Osteopontin	60.8 ± 15.70	102.85 ± 29.02	0.216
F19-20	Osteoprotegerin	46 ± 45.20	54.13 ± 28.75	0.852
F21-22	PDGF-BB	730.47 ± 114.39	505.6 ± 84.87	0.155
F23-24	Pref-1	9.45 ± 13.36	33.38 ± 47.20	0.562
G05-06	RBP4	110.31 ± 55.24	234.5 ± 19.80	0.096
G07-08	Resistin	283.37 ± 176.86	531.19 ± 103.63	0.229
G21-22	VCAM-1	103.92 ± 22.36	226.59 ± 22.58	0.032* A

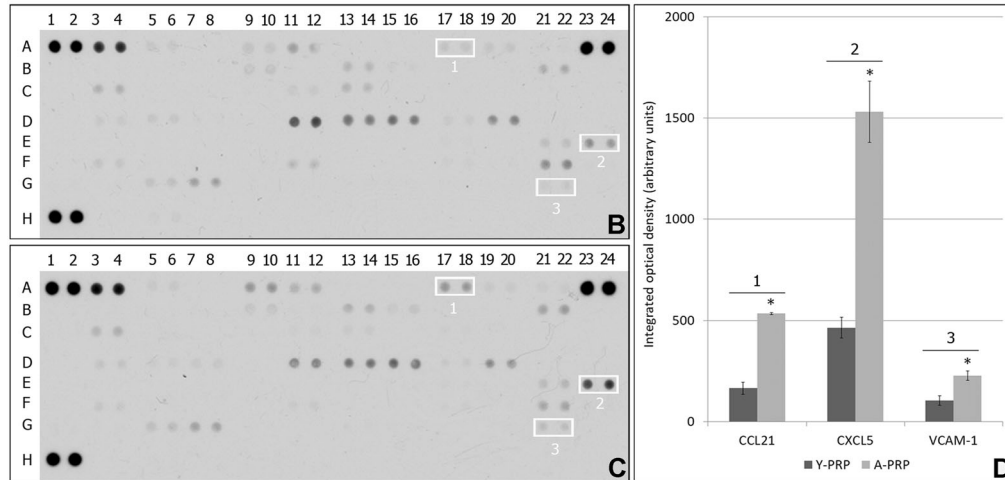


**FIGURE 1** Molecular analysis of platelet-rich plasma (PRPs). A, List of molecules detected in the analysis. B, Cytokine array of Y-PRP. C, Cytokine array of A-PRP. D, Most incremented molecular levels in the A-PRP with respect to the Y-PRP; Y-PRP, young PRP group; A-PRP, aged PRP group; 1, CCL21; 2, CXCL5; 3, VCAM-1. \*P < .05 with regard to Y-PRP. Error bars = standard deviation

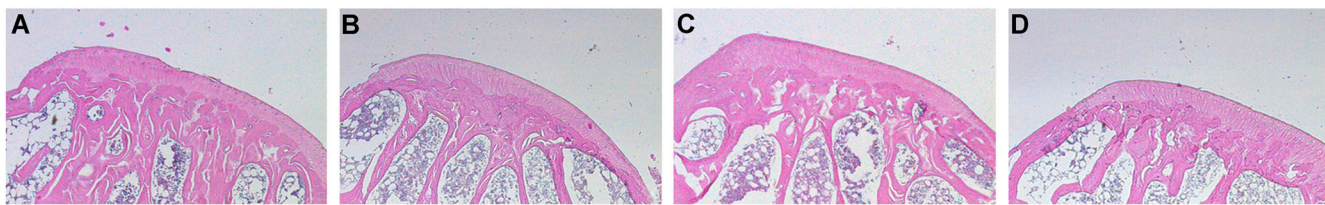


**FIGURE 2** Histological analysis of femur condyle cartilage. A, Control group. B, Saline group. C, Young PRP group. D, Aged PRP group. PRP, platelet-rich plasma [Color figure can be viewed at [wileyonlinelibrary.com](#)]

viability, subchondral bone, and cartilage mineralization according to ICRS score (Table 1).

Histological analysis of the longitudinal femoral samples revealed differences in the bone diaphysis. The groups treated with PRP showed a similar percentage of cellularity in the bone marrow, being  $59.94\% \pm 4.83\%$  in the A-PRP group and  $60.08\% \pm 7.08\%$  in the Y-PRP group. However, both groups treated with PRP did show greater cellularity ( $P < .05$ ) with respect to the untreated group ( $46.98\% \pm 4.79\%$ ) and the group treated with intraosseous saline injections ( $48.83\% \pm 6.88\%$ ) (Figure 3).

Concerning vastus lateralis samples, groups treated with PRP showed less collagen than the control group treated with saline. In fact, the Y-PRP group had the lowest percentage of collagen ( $5.65\% \pm 4.00\%$ ) compared with the A-PRP group ( $7.69\% \pm 3.90\%$ ) as well as the two control groups ( $10.58\% \pm 5.58\%$  for saline and  $10.19\% \pm 6.78\%$  for untreated group) (Figure 4).

### 3.3 | micro-CT analysis

The values resulting from the micro-CT analysis are shown in Table 2. Concerning cortical bone, no differences between any group in volume and intensity were found in any of the regions analyzed ( $P > .05$ ). When the trabecular bone was analyzed, the group treated with PRP from young donors (Y-PRP group) had less space between the trabeculae ( $P < .05$ ) and a higher trabecular density ( $P < .05$ ) in the distal metaphysis (Figure 5). In addition, the Y-PRP group also showed a higher percentage of trabecular occupation ( $P < .05$ ) in the distal metaphysis as well as in the distal epiphysis. A higher volume of

the femoral condyle subchondral plate was observed ( $P < .05$ ) in the Y-PRP group.

## 4 | DISCUSSION

Although clinical studies have achieved promising results by means of intraosseous infiltrations of PRP, their biological effects have not been studied yet. In this work, we evaluated for the first time the effect of intraosseous infiltrations of two different types of PRP based on the age of donors, achieving better biological and structural results than the two control groups. One of these controls received saline infiltrations to differentiate between the biologic effects of PRP and the mechanical effects due to the injections. It is worth mentioning that, although both PRPs had a composition with a similar number of platelets and no leukocytes or erythrocytes, these results were more pronounced in the group treated with PRP from young donors.

The effects produced after intraosseous infiltrations of PRP were analyzed histologically in tissues where the local action of this therapy could be manifested reasonably. Thus, in the bone marrow of the femurs where treatments were administered directly, the groups that received PRP had greater cellularity whereas both control groups showed an increase in adipogenicity. This natural process, in which the increase in adipogenesis of the bone marrow is detrimental to the cellularity and bone mass,<sup>17</sup> is in accordance with our aged animal model since the control group showed a considerable number of adipocytes. However, the groups that received PRP treatment from both young and elderly donors presented approximately 15%

**TABLE 1** ICRS visual histological assessment

	C group (mean $\pm$ sd)	S group (mean $\pm$ sd)	Y-PRP group (mean $\pm$ sd)	A-PRP group (mean $\pm$ sd)	P value
1. Surface	$0.50 \pm 1.22$	$1.00 \pm 1.55$	$1.20 \pm 1.64$	$1.20 \pm 1.64$	.846
2. Matrix	$2.67 \pm 0.52$	$3.00 \pm 0.00$	$3.00 \pm 0.00$	$2.80 \pm 0.45$	.309
3. Cell distribution	$2.00 \pm 0.89$	$2.17 \pm 0.41$	$2.60 \pm 0.55$	$2.40 \pm 0.55$	.443
4. Cell viability	$2.67 \pm 0.52$	$2.83 \pm 0.41$	$3.00 \pm 0.00$	$3.00 \pm 0.00$	.347
5. Subchondral bone	$2.50 \pm 0.55$	$2.50 \pm 0.55$	$2.80 \pm 0.45$	$2.80 \pm 0.45$	.599
6. Cartilage mineralization	$2.83 \pm 0.41$	$2.83 \pm 0.41$	$3.00 \pm 0.00$	$3.00 \pm 0.00$	.657

Abbreviations: A-PRP, aged PRP; C, control; ICRS, International Cartilage Repair Society; PRP, platelet-rich plasma; S, saline; sd, standard deviation; Y-PRP, young PRP.

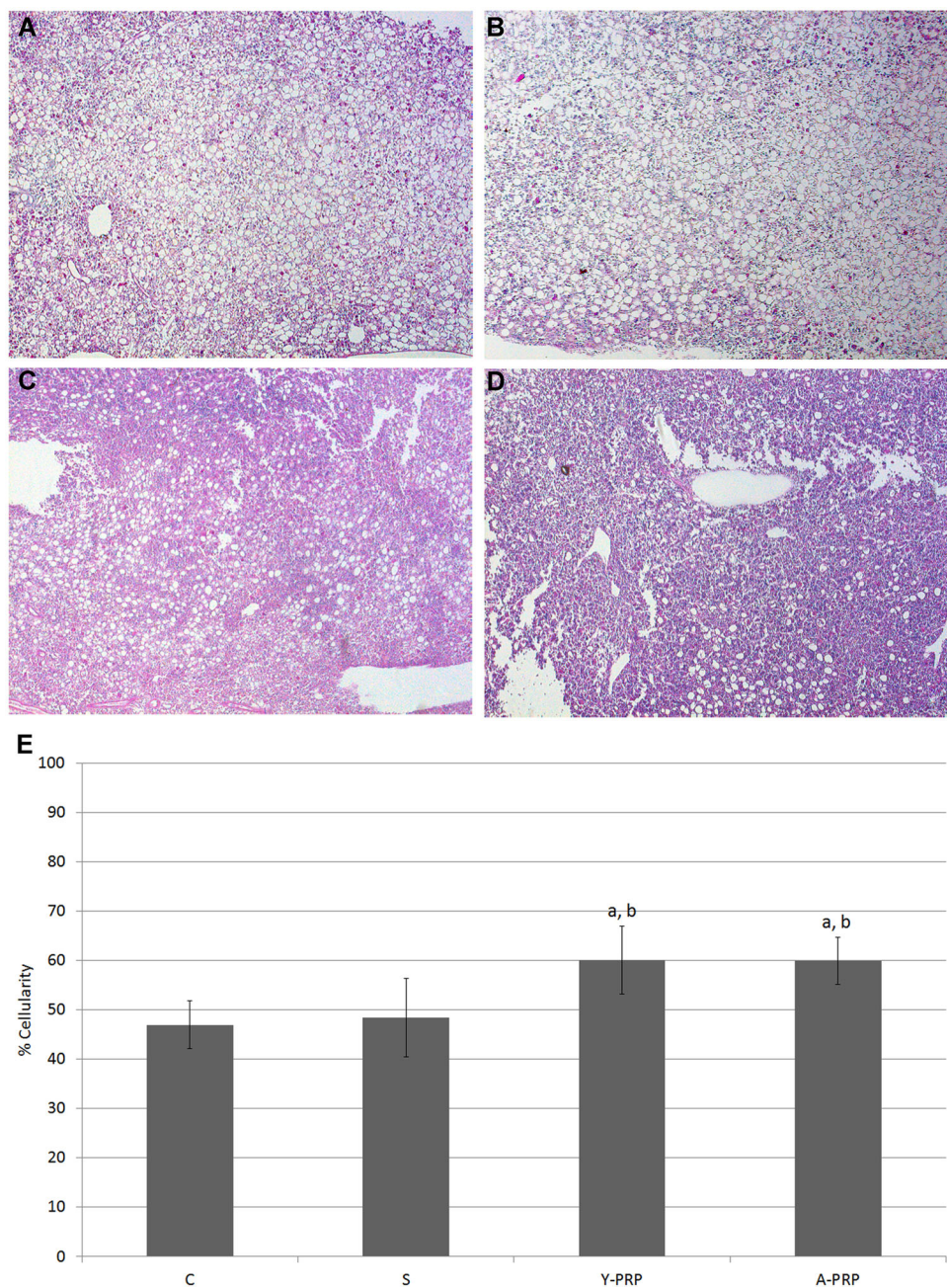


**FIGURE 3** Histological analysis of the femur bone marrow. A, Control group. B, Saline group. C, Young PRP group. D, Aged PRP group. E, Cellularity levels (%). A-PRP, aged PRP group; C, control group; PRP, platelet-rich plasma; S, Saline group; Y-PRP, young PRP group. <sup>a</sup>P < .05 with regard to C group; <sup>b</sup>P < .05 with regard to S group [Color figure can be viewed at [wileyonlinelibrary.com](http://wileyonlinelibrary.com)]

less adiposity, suggesting some biological effects able to slow down this aging process.

Because of that increase of adipose accumulation in the bone marrow there is a loss of bone that has been reported by several studies<sup>18</sup> and also a decrease in trabecular bone volume.<sup>11</sup> The adipose invasion of the bone marrow and the consequent loss of bone occurs under physiological conditions such as normal aging<sup>19</sup> and pathological processes such as osteoporosis.<sup>20</sup> Consistent with these findings, micro-CT analysis performed in this study showed better bone structure in the groups treated with PRP, and

significantly in the group treated with PRP from young donors. Although these differences were not observed in the cortical bone, a superior occupation and density of the trabecular bone were found not only in the metaphysis, which is the area where these changes are usually more relevant,<sup>21</sup> but also in the epiphysis. Considering parameters such as trabecular space, thickness, and density, the higher trabecular occupation observed is related to a greater number of trabeculae compared to the control group. Aging is also a cause of the decrease of the trabecular number, as demonstrated in other studies. In a work carried out by Jimenez-Andrade et al.,<sup>22</sup>

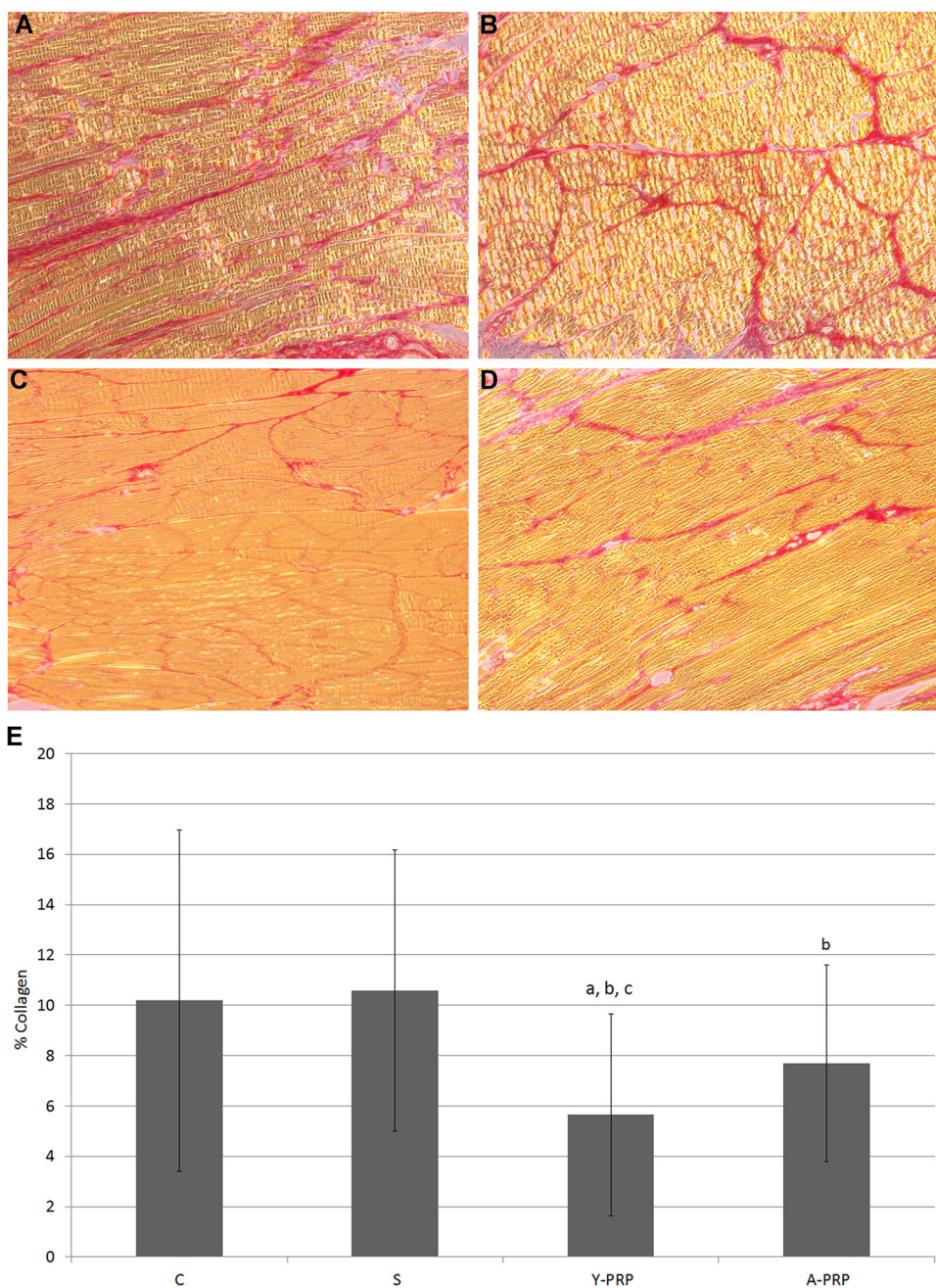


**FIGURE 4** Histological analysis of the vastus lateralis. A, Control group. B, Saline group. C, Young PRP group. D, Aged PRP group. E, Collagen levels (%). A-PRP, aged PRP group; C, control group; PRP, platelet-rich plasma; S, saline group, Y-PRP, young PRP group. <sup>a</sup>P < .05 with regard to C group; <sup>b</sup>P < .05 with regard to S group; <sup>c</sup>P < .05 with regard to A-PRP group [Color figure can be viewed at [wileyonlinelibrary.com](http://wileyonlinelibrary.com)]

micro-CT images of the distal metaphysis showed an age-related reduction in trabecular number comparing femurs from young, middle-aged and old male rats. Therefore, our histological and micro-CT results suggest a preventive action of the PRP to physiological processes such as aging.

Another finding after the bone analysis was a higher volume of the subchondral plate in the Y-PRP group. Several studies related the thinning of the subchondral plate with the early development of osteoarthritis.<sup>23</sup> The authors showed that using different osteoarthritic models the subchondral plate thickness was reduced

regardless of the load conditions and the cartilage damage, confirming that it is a common initial process to the development of osteoarthritis.<sup>24,25</sup> The animals used in the present work were not osteoarthritic models, which was confirmed with high values in the ICRS score in all groups. Nevertheless, it could mean the development of early osteoarthritis that has not yet been translated into cartilage damage and that is preceded by thinning of the subchondral in all groups except for the Y-PRP group.

One of the main possible causes of the histological and structural changes observed in this work is inflammation either related to aging<sup>26</sup>

**TABLE 2** Micro-computed tomography values

	C group (mean ± sd)	S group (mean ± sd)	Y-PRP group (mean ± sd)	A-PRP group (mean ± sd)	P value
<b>Diaphysis</b>					
CB Vol, mm <sup>3</sup>	259.08 ± 18.19	267.32 ± 37.09	274.05 ± 38.40	294.73 ± 17.01	.266
CB Int	58.57 ± 4.51	193.47 ± 4.34	191.89 ± 5.33	194.39 ± 3.18	.496
<b>Distal metaphysis</b>					
CB Vol, mm <sup>3</sup>	58.57 ± 6.34	54.01 ± 10.94	55.94 ± 10.49	62.99 ± 14.91	.575
CB Int	175.70 ± 3.96	173.16 ± 5.00	169.39 ± 5.06	174.45 ± 2.52	.132
TB Vol, mm <sup>3</sup>	14.43 ± 1.99	14.67 ± 3.26	18.26 ± 3.69	16.99 ± 3.8	.181
TB occup (%)	18.29 ± 1.45	18.97 ± 3.27	25.26 ± 3.55 <sup>a,b</sup>	22.01 ± 3.79	.006
TB Th Mean, mm	0.14 ± 0.02	0.14 ± 0.03	0.15 ± 0.01	0.14 ± 0.01	.721
TB Th Max, mm	0.43 ± 0.06	0.45 ± 0.09	0.48 ± 0.04	0.46 ± 0.11	.745
TB Sp Mean, mm	0.98 ± 0.10	0.82 ± 0.09	0.65 ± 0.12 <sup>a,b</sup>	0.80 ± 0.25	.018
TB Sp Max, mm	2.35 ± 0.37	1.90 ± 0.29	1.74 ± 0.33	1.93 ± 0.53	.086
Density, kg/mm <sup>3</sup>	0.82 ± 0.23	1.07 ± 0.33	1.43 ± 0.30 <sup>a</sup>	1.16 ± 0.43	.044
<b>Distal epiphysis</b>					
TB Vol, mm <sup>3</sup>	59.71 ± 4.44	68.21 ± 13.79	60.10 ± 6.92	61.95 ± 7.08	.361
TB occup (%)	65.97 ± 1.70	66.43 ± 4.46	71.79 ± 3.1 <sup>a</sup>	67.92 ± 3.45	.043
TB Th Mean, mm	0.36 ± 0.02	0.37 ± 0.06	0.39 ± 0.04	0.39 ± 0.03	.499
TB Th Max, mm	0.89 ± 0.11	0.96 ± 0.13	0.99 ± 0.13	0.94 ± 0.08	.561
TB Sp Mean, mm	0.66 ± 0.04	0.69 ± 0.08	0.66 ± 0.05	0.70 ± 0.08	.694
TB Sp Max, mm	1.69 ± 0.15	1.74 ± 0.17	1.70 ± 0.23	1.80 ± 0.2	.747
Density, kg/mm <sup>3</sup>	1.69 ± 0.40	1.58 ± 0.34	1.72 ± 0.61	1.37 ± 0.15	.510
<b>Subchondral plate</b>					
Vol, mm <sup>3</sup>	0.68 ± 0.16	0.75 ± 0.25	1.28 ± 0.29 <sup>a,b,c</sup>	0.68 ± 0.31	.003

Abbreviations: A-PRP, aged PRP; C, control; CB Int, cortical bone intensity; CB Vol, cortical bone volume; PRP, platelet-rich plasma; S, saline; TB occup, trabecular bone occupation; TB Sp Max, trabecular bone maximum space; TB Sp Mean, trabecular bone mean space; TB Th Max, trabecular bone maximum thickness; TB Th Mean, trabecular bone mean thickness; TB Vol, trabecular bone volume; Vol, volume; Y-PRP, young PRP.

<sup>a</sup>P < .05 with regard to C group.

<sup>b</sup>P < .05 with regard to S group.

<sup>c</sup>P < .05 with regard to the A-PRP group.

or to the development of pathologies such as osteoarthritis.<sup>27,28</sup> An inflammatory environment in the bone marrow favors its replacement with adipose tissue, and consequently the future alterations of the bone microarchitecture. With aging, the accumulation in the bone marrow of reactive oxygen species promotes the induction of nuclear factor kappa B (NF-κB) which is one of the most important mediating pathways in inflammation.<sup>29</sup> The activation of this pathway causes the production of proinflammatory molecules that create a proinflammatory environment and consequently a series of molecular and cellular signals that favor the age-associated shift from osteogenesis to adipogenesis.<sup>13,30</sup> It is precisely in this process where PRP acts since its anti-inflammatory action is carried out through the inhibition of the NF-κB pathway. Yin et al<sup>13</sup> observed in an in vitro study that the therapeutic action of PRP over human bone marrow-derived mesenchymal stem cells lied in part in the suppression of the NF-κB pathway. The effect of PRP on this inflammatory pathway was also confirmed in an in vivo study in which cartilage regeneration was evaluated.<sup>31</sup> The mechanism by which the PRP carries out its inhibitory action of the NF-κB pathway is related to growth factors present in it such as HGF,<sup>32</sup> which was detected in the molecular analysis of the PRPs administered in the present work. Therefore, the intraosseous administration of PRP could modulate the

inflammatory processes present in the bone marrow suppressing the NF-κB pathway, avoiding adipogenesis and as a result preventing changes in the bone structure associated with age or other pathologies.

It should be noted that although groups treated with a PRP presented lower adipogenesis of the bone marrow, bone architecture was more favorable in the group treated with PRP from young donors. The enhancement of the effects generated in the Y-PRP group could be justified by the differences at the molecular level since the cellular composition was similar. Indeed, after the molecular analysis of both PRPs and according to previous studies,<sup>33</sup> we observed that the PRP of aged donors had a more proinflammatory profile, showing a higher level in some cytokines namely, CCL21 and CXCL5. Besides its proinflammatory nature, several authors reported these two molecules are also related to osteoclastogenesis, which is also activated by NF-κB pathway after induction of RANK ligand by CXCL5.<sup>30,31,34,35</sup> Thus, the higher levels of proinflammatory molecules and with stimulation of bone resorption may decrease the PRP effect of aged donors, although they still maintain their anti-inflammatory properties. These results are consistent with other studies in which PRPs rich in proinflammatory showed less efficacy due to activation of the NF-κB pathway (Figure 6).<sup>13,14</sup>

**FIGURE 5** Three-dimensional rendered images of the femur metaphysis from (A) control group, (B) saline group, (C) young PRP group, and (D) aged PRP Group.

Micro-computed tomography images of the femur from (E) control group, (F) saline group, (G) young PRP group and (H) aged PRP group. PRP, platelet-rich plasma [Color figure can be viewed at [wileyonlinelibrary.com](http://wileyonlinelibrary.com)]

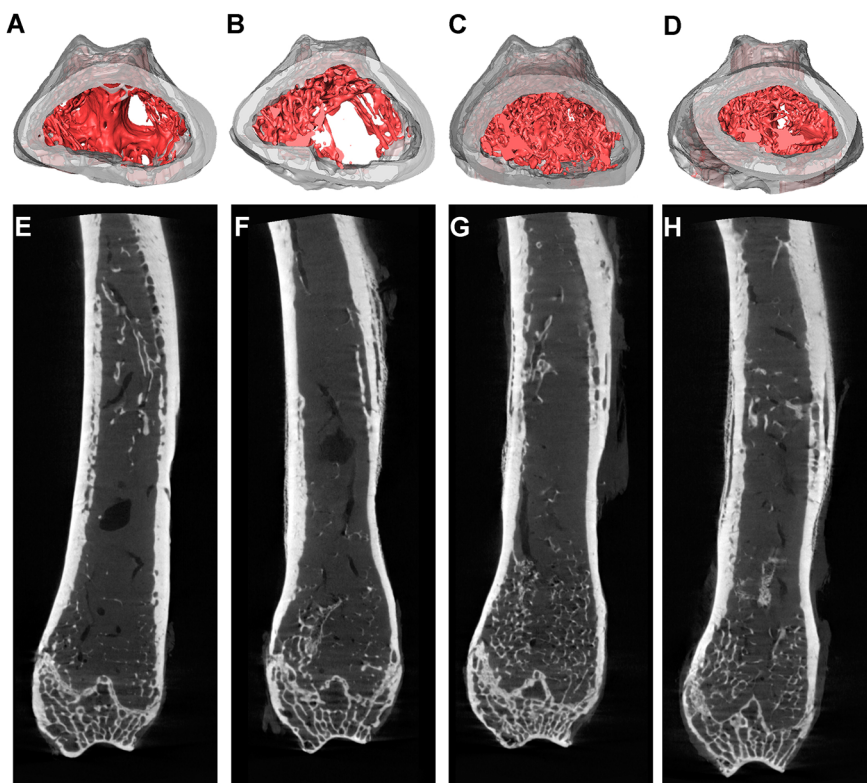
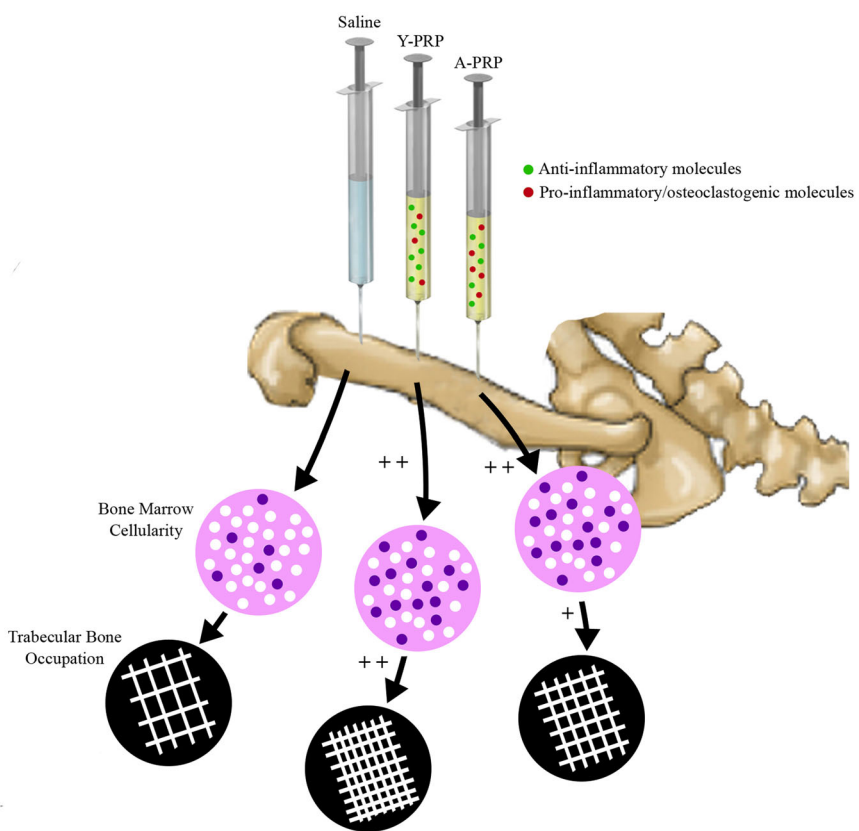


**FIGURE 6** Schematic representation of the platelet-rich plasma (PRP) action. The anti-inflammatory effect of PRP may prevent processes of adipogenesis and osteoclastogenesis in the bone marrow and consequently prevents the loss of trabecular bone. Because the levels of proinflammatory and/or osteoclastogenic molecules are higher in the PRP from aged donors, its therapeutic effect may be diminished in comparison with the PRP from young donors. A-PRP, aged PRP; Y-PRP, young PRP [Color figure can be viewed at [wileyonlinelibrary.com](http://wileyonlinelibrary.com)]



Animals treated with PRP from young donors also showed a greater effect in the repair of muscle tissue adjacent to the femur, which was damaged during surgeries. The PRP groups showed a better repair than the control groups according to the lower presence of fibrosis in this tissue.<sup>36</sup> However, these findings also showed a better reparative activity of PRP from young donors. The results obtained suggest continuing in the lines of research related to the use of allogeneic PRPs that most favor the biological processes and lead to tissue repair. These studies should evaluate not only the therapeutic potential of these allogenic PRPs but also the aspects related to immune reactions due to the presence of other cell populations such as leukocytes in some of the PRP types. Some authors showed promising results in clinical studies in patients with osteoarthritis and they did not report immunity issues.<sup>37</sup>

## 5 | CONCLUSION

In summary, the present work showed the biological action of PRP in the bone marrow after intraosseous infiltrations. This effect was greater after the PRP application of young donors with a less inflammatory profile than PRP from aged donors. Its administration favors an anti-inflammatory environment into the bone marrow that prevents the adipogenesis and osteoclastogenesis associated with aging and possible pathologies, maintaining consequently a healthier bone structure. These findings can be transferred to the clinic to explain the clinical results that are being achieved with this technique as well as to apply in cases where the maintenance of osteoarticular homeostasis helps in the treatment of patients. Finally, further studies will be needed in order to increase our knowledge about PRP and its therapeutic potential.

## ACKNOWLEDGMENTS

This work was supported by the Provincial Council of Alava through the AlavalInnova Program and Basque Government through the HAZITEK Program. The authors wish to thank C. Ortiz de Solorzano, X. Morales, and M. Ariz (Imaging Platform, CIMA, Universidad de Navarra) for their Micro-computed tomography technical support, and CNB Histology Service for their histology technical support.

## CONFLICT OF INTERESTS

The authors declare that there are no conflict of interests.

## AUTHOR CONTRIBUTIONS

DD, AG, PS, AMB, and MS contributed to the conception and design of the study. DD, AG, PS, GG, and JS contributed to the provision of study materials and animals, and to the performance of treatments and sacrifices. DD, AG, AMB, GG, JS, and MS contributed to the analysis and interpretation of the data. DD, AG, PS, GG, JS, and MS contributed to drafting, writing, critical revision, and final approval of the article. All authors have read and approved the final submitted manuscript.

## DATA AVAILABILITY STATEMENT

The raw/processed data required to reproduce these findings cannot be shared at this time due to technical or time limitations. However, they can be provided upon request.

## ORCID

Diego Delgado  <http://orcid.org/0000-0002-0494-0804>

Gontzal García del Caño  <http://orcid.org/0000-0002-7098-0986>

Mikel Sánchez  <http://orcid.org/0000-0001-9992-6927>

## REFERENCES

1. Lepage SIM, Robson N, Gilmore H, et al. Beyond cartilage repair: the role of the osteochondral unit in joint health and disease. *Tissue Eng Part B Rev.* 2019;25(2):114-125.
2. Karsdal MA, Bay-Jensen AC, Lories RJ, et al. The coupling of bone and cartilage turnover in osteoarthritis: opportunities for bone anti-resorptives and anabolics as potential treatments? *Ann Rheum Dis.* 2014;73(2):336-348.
3. Zhao W, Wang T, Luo Q, et al. Cartilage degeneration and excessive subchondral bone formation in spontaneous osteoarthritis involves altered TGF- $\beta$  signaling. *J Orthop Res.* 2016;34(5):763-770.
4. DeLong JM, Russell RP, Mazzocca AD. Platelet-rich plasma: the PAW classification system. *Arthroscopy.* 2012;28(7):998-1009.
5. Han Y, Huang H, Pan J, et al. Meta-analysis comparing platelet-rich plasma vs hyaluronic acid injection in patients with knee osteoarthritis. *Pain Med.* 2019;20:1418-1429.
6. Xing D, Wang B, Zhang W, et al. Intra-articular platelet-rich plasma injections for knee osteoarthritis: an overview of systematic reviews and risk of bias considerations. *Int J Rheum Dis.* 2017;20(11):1612-1630.
7. Sánchez M, Anitua E, Delgado D, et al. A new strategy to tackle severe knee osteoarthritis: combination of intra-articular and intraosseous injections of platelet rich plasma. *Expert Opin Biol Ther.* 2016;16(5):627-643.
8. Delgado D, Garate A, Vincent H, et al. Current concepts in intraosseous platelet-rich plasma injections for knee osteoarthritis. *J Clin Orthop Trauma.* 2019;10(1):36-41.
9. Sánchez M, Delgado D, Sánchez P, et al. Combination of intra-articular and intraosseous injections of platelet rich plasma for severe knee osteoarthritis: a pilot study. *BioMed Res Int.* 2016;2016:4868613.
10. Justesen J, Stenderup K, Ebbesen EN, Mosekilde L, Steiniche T, Kassem M. Adipocyte tissue volume in bone marrow is increased with aging and in patients with osteoporosis. *Biogerontology.* 2001;2(3):165-171.
11. Costa S, Fairfield H, Reagan MR. Inverse correlation between trabecular bone volume and bone marrow adipose tissue in rats treated with osteoanabolic agents. *Bone.* 2019;123:211-223.
12. Larsson A, Carlsson L, Gordh T, Lind AL, Thulin M, Kamali-Moghaddam M. The effects of age and gender on plasma levels of 63 cytokines. *J Immunol Methods.* 2015;425:58-61.
13. Xu Z, Yin W, Zhang Y, et al. Comparative evaluation of leukocyte- and platelet-rich plasma and pure platelet-rich plasma for cartilage regeneration. *Sci Rep.* 2017;7:43301.
14. Yin W, Qi X, Zhang Y, et al. Advantages of pure platelet-rich plasma compared with leukocyte- and platelet-rich plasma in promoting repair of bone defects. *J Transl Med.* 2016;14:73.
15. Schneider CA, Rasband WS, Eliceiri KW. NIH Image to ImageJ: 25 years of image analysis. *Nat Methods.* 2012;9(7):671-675.
16. Doube M, Kłosowski MM, Arganda-Carreras I, et al. BoneJ: free and extensible bone image analysis in ImageJ. *Bone.* 2010;47(6):1076-1079.
17. Baker J, Nederveen JP, Ibrahim G, Ivankovic V, Joannisse S, Parise G. Exercise training differentially alters axial and appendicular marrow cellularity in old mice. *Appl Physiol Nutr Metab.* 2018;43(5):523-527.

18. Li J, Liu X, Zuo B, Zhang L. The role of bone marrow microenvironment in governing the balance between osteoblastogenesis and adipogenesis. *Aging Dis.* 2015;7(4):514-525.
19. Hartsock RJ, Smith EB, Petty CS. Normal variations with aging of the amount of hematopoietic tissue in bone marrow from the anterior iliac crest. A study made from 177 cases of sudden death examined by necropsy. *Am J Clin Pathol.* 1965;43:326-331.
20. Meunier P, Aaron J, Edouard C, Vignon G. Osteoporosis and the replacement of cell populations of the marrow by adipose tissue. A quantitative study of 84 iliac bone biopsies. *Clin Orthop Relat Res.* 1971;80:147-154.
21. Zhang HW, Ding J, Jin JL, et al. Defects in mesenchymal stem cell self-renewal and cell fate determination lead to an osteopenic phenotype in Bmi-1 null mice. *J Bone Miner Res.* 2010;25(3):640-652.
22. Jimenez-Andrade JM, Mantyh WG, Bloom AP, et al. The effect of aging on the density of the sensory nerve fiber innervation of bone and acute skeletal pain. *Neurobiol Aging.* 2012;33(5):921-932.
23. Florea C, Malo MKH, Rautainen J, et al. Alterations in subchondral bone plate, trabecular bone and articular cartilage properties of rabbit femoral condyles at 4 weeks after anterior cruciate ligament transection. *Osteoarthritis Cartilage.* 2015;23(3):414-422.
24. Botter SM, van Osch GJVM, Waarsing JH, et al. Cartilage damage pattern in relation to subchondral plate thickness in a collagenase-induced model of osteoarthritis. *Osteoarthritis Cartilage.* 2008;16(4):506-514.
25. Snijders YH, Intema F, Lafeber FP, et al. A role for subchondral bone changes in the process of osteoarthritis; a micro-CT study of two canine models. *BMC Musculoskelet Disord.* 2008;9:20.
26. Baylis D, Bartlett DB, Patel HP, Roberts HC. Understanding how we age: insights into inflammaging. *Longev Healthspan.* 2013;2(1):8.
27. Berenbaum F. Osteoarthritis as an inflammatory disease (osteoarthritis is not osteoarthrosis!). *Osteoarthritis Cartilage.* 2013;21(1):16-21.
28. Jaswal AP, Bandyopadhyay A. Re-examining osteoarthritis therapy from a developmental biologist's perspective. *Biochem Pharmacol.* 2019;S0006-2952(19). 30106-30106.
29. Chung HY, Sung B, Jung KJ, Zou Y, Yu BP. The molecular inflammatory process in aging. *Antioxid Redox Signal.* 2006;8(3-4):572-581.
30. Takeshita S, Fumoto T, Naoe Y, Ikeda K. Age-related marrow adipogenesis is linked to increased expression of RANKL. *J Biol Chem.* 2014;289(24):16699-16710.
31. Lee J, Park C, Kim HJ, et al. Stimulation of osteoclast migration and bone resorption by C-C chemokine ligands 19 and 21. *Exp Mol Med.* 2017;49(7):e358.
32. Bendinelli P, Matteucci E, Dogliotti G, et al. Molecular basis of anti-inflammatory action of platelet-rich plasma on human chondrocytes: mechanisms of NF-κB inhibition via HGF. *J Cell Physiol.* 2010;225:757-766.
33. Stowe RP, Peek MK, Cutchin MP, Goodwin JS. Plasma cytokine levels in a population-based study: relation to age and ethnicity. *J Gerontol A Biol Sci Med Sci.* 2010;65A(4):429-433.
34. Boyce BF, Xiu Y, Li J, Xing L, Yao Z. NF-κB-mediated regulation of osteoclastogenesis. *Endocrinol Metab.* 2015;30(1):35-44.
35. Sundaram K, Rao DS, Ries WL, Reddy SV. CXCL5 stimulation of RANK ligand expression in Paget's disease of bone. *Lab Invest.* 2013;93(4):472-479.
36. Garcia TA, Camargo RCT, Koike TE, Ozaki GAT, Castoldi RC, Camargo Filho JCS. Histological analysis of the association of low level laser therapy and platelet-rich plasma in regeneration of muscle injury in rats. *Braz J Phys Ther.* 2017;21(6):425-433.
37. Bottegoni C, Dei Giudici L, Salvemini S, Chiurazzi E, Bencivenga R, Gigante A. Homologous platelet-rich plasma for the treatment of knee osteoarthritis in selected elderly patients: an open-label, uncontrolled, pilot study. *Ther Adv Musculoskelet Dis.* 2016;8(2):35-41.

## SUPPORTING INFORMATION

Additional supporting information may be found online in the Supporting Information section.

**How to cite this article:** Delgado D, Garate A, Sánchez P, et al. Biological and structural effects after intraosseous infiltrations of age-dependent platelet-rich plasma: An in vivo study. *J Orthop Res.* 2020;1-11.  
<https://doi.org/10.1002/jor.24646>